HHS Public Access

Author manuscript

Proteins. Author manuscript; available in PMC 2020 May 01.

Published in final edited form as:

Proteins. 2020 May ; 88(5): 689–697. doi:10.1002/prot.25853.

Design and characterization of novel dual Fc antibody with enhanced avidity for Fc receptors

Dennis R. Goulet[1], **Adam Zwolak**[2], **James A. Williams**[1], **Mark L. Chiu**[2], **William M. Atkins**[1]

[1]Department of Medicinal Chemistry, University of Washington, Seattle, Washington

[2]Biologics Research, Janssen Research & Development, Spring House, Pennsylvania

Abstract

Monoclonal antibodies (mAbs) have become an important class of therapeutics, particularly in the realm of anticancer immunotherapy. While the two antigen-binding fragments (Fabs) of an mAb allow for high-avidity binding to molecular targets, the crystallizable fragment (Fc) engages immune effector elements. mAbs of the IgG class are used for the treatment of autoimmune diseases and can elicit antitumor immune functions not only by several mechanisms including direct antigen engagement via their Fab arms but also by Fab binding to tumors combined with Fc engagement of complement component C1q and Fcγ receptors. Additionally, IgG binding to the neonatal Fc receptor (FcRn) allows for endosomal recycling and prolonged serum half-life. To augment the effector functions or half-life of an IgG1 mAb, we constructed a novel "2Fc" mAb containing two Fc domains in addition to the normal two Fab domains. Structural and functional characterization of this 2Fc mAb demonstrated that it exists in a tetrahedral-like geometry and retains binding capacity via the Fab domains. Furthermore, duplication of the Fc region significantly enhanced avidity for Fc receptors FcγRI, FcγRIIIa, and FcRn, which manifested as a decrease in complex dissociation rate that was more pronounced at higher densities of receptor. At intermediate receptor density, the dissociation rate for Fc receptors was decreased 6- to 130-fold, resulting in apparent affinity increases of 7- to 42-fold. Stoichiometric analysis confirmed that each 2Fc mAb may simultaneously bind two molecules of FcγRI or four molecules of FcRn, which is double the stoichiometry of a wild-type mAb. In summary, duplication of the IgG Fc region allows for increased avidity to Fc receptors that could translate into clinically relevant enhancement of effector functions or pharmacokinetics.

Keywords

antibody avidity; antibody-dependent cell cytotoxicity; immunotherapy; monoclonal antibodies; pharmacokinetics; protein engineering

Correspondence William M. Atkins, Department of Medicinal Chemistry, University of Washington, Seattle, WA 98195-7610.winky@uw.edu.

SUPPORTING INFORMATION

Additional supporting information may be found online in the Supporting Information section at the end of this article.

Peer Review

The peer review history for this article is available at https://publons.com/publon/10.1002/prot.25853.

CONFLICT OF INTERESTS

The authors declare that they have no conflict of interest.

1 | INTRODUCTION

Monoclonal antibody (mAb)-based, and in particular immunoglobulin G (IgG)-based, therapeutics have become an extremely successful class of drugs due to the potency, specificity, stability, and adaptability of the mAb framework.[1,2] Based on their role in adaptive immunity, Abs have an intrinsic ability to interact with other elements of the immune system. Thus, therapeutic mAbs can be used to treat autoimmune diseases and elicit an anticancer immune response by directing leukocytes and other humoral factors to target specific antigen-expressing cells.[3,4] Clinically, the most important IgG effector functions are complement-dependent cytotoxicity (CDC), antibody-dependent cellular phagocytosis (ADCP), and antibody-dependent cell-mediated cytotoxicity (ADCC), with each mechanism eliciting a distinct immune program for elimination of target cells.[5] Of these, CDC requires binding of hexameric IgG mAb clusters on the target cell to C1q protein, which is the first component of the complement cascade. ADCP and ADCC rely on IgG crystallizable fragment (Fc) binding to Fcγ receptors (FcγRs) expressed on phagocytes and natural killer (NK) cells, respectively. Binding of mAbs to antigen-bearing target cells via their two antigen-binding fragments (Fabs) and to FcγRs via the Fc leads to cross-linking of FcγRs and downstream transcriptional changes associated with effector cell activation. Besides C1q and FcγRs, IgG mAbs also bind the neonatal Fc receptor (FcRn) at the acidic pH of the recycling endosome, which rescues them from lysosomal degradation and confers them with their characteristically long serum half-lives.[6]

Numerous protein engineering efforts have focused on modulating effector function by altering Fc interactions with FcγRs.[7,8] Elimination of ADCP and ADCC can be achieved by abrogating Fc-FcγR binding and is desirable for mAbs whose intended therapeutic mechanism is simple inhibition of antigen function.[9,10] Conversely, enhancement of these effector functions can be beneficial for anticancer therapeutics and is achieved by amplifying IgG activation of effector cells. For example, amino acid substitutions of the Fc that lead to higher affinity for FcγRIIIa result in enhanced ADCC.[11–13] However, incorporation of novel mutations has notable drawbacks including the possibility of decreased stability and increased immunogenicity.[14,15] The glycan profile of IgG mAbs has also been linked to their immune functions, with low fucose IgG glycoforms having improved binding to FcγRIIIa and more potent ADCC.[16]

A less established strategy for modulation of effector mechanisms is the duplication of the entire Fc CH2-CH3 domains. This Fc multimerization strategy has already proven effective for CDC, where Fc mutations favoring noncovalent IgG hexamerization upon antigen binding result in more potent complement-mediated lysis of target cells.[17,18] Regarding ADCP and ADCC, incorporation of multiple Fc domains into each IgG molecule may amplify FcγR signaling by strengthening the avidity of the Fc-FcγR interaction or by facilitating FcγR cross-linking. In fact, studies with IgG variants containing two or three tandemly repeated Fc domains have shown enhanced FcγR-mediated effector function compared to the wild-type IgG.[19–21] However, avidity effects are expected to be a function not only of the number of binding elements but also of their three-dimensional arrangement. Avidity could vary between constructs with the same number of Fc regions, but with different structural topologies.

Here, an alternative IgG scaffold with distinct structural geometry is presented. Fc and Fab regions were arranged into a “tetrahedral” format to maximize bivalent binding to both antigens and FcγRs and therefore allow more efficient lymphocyte recruitment. Biochemical and structural characterization combined with detailed kinetic analysis of FcR binding mechanism demonstrate the successful modulation of receptor-binding avidity with potential therapeutic implications.

2 | MATERIALS AND METHODS

2.1 | Proteins

Wild-type human IgG1 mAbs (antirespiratory syncytial virus [anti-RSV], clone B21M) containing a single Fc sequence were expressed transiently in Expi293F cells (Thermo Fisher, A14635) using a 3:1 ratio of light chain (LC) to heavy chain (HC) DNA according to the manufacturer’s instructions. For dual Fc variants, plasmids containing the LC -Fc fusion were used in place of normal LC plasmids, with a 1:1 ratio of HC and LC-Fc fusion DNA. The DNA sequence for the LC-Fc fusion used the entire LC sequence immediately followed by the HC sequence, beginning at the “DKTHTCPPCP” motif of the hinge and continuing to the end of the HC. mAbs were purified using a MabSelect SuRe column (GE Life Sciences, 29049104) according to the manufacturer’s protocol, followed immediately by Size-exclusion chromatography (SEC) using a Superdex 200 10/300 GL column (GE Life Sciences, 17517501) in ×1 phosphate-buffered saline (PBS; 2.67 mM KCl, 1.47 mM KH_2PO_4, 138 mM NaCl, and 8.06 mM Na_2HPO_4), pH 7.2. Analytical SEC to characterize purified protein was run analogously, loading 20 μg of protein onto the column. Denaturing polyacrylamide gel electrophoresis (SDS-PAGE) was performed using a BioRad Protean TGX 4–15% acrylamide gel, Tris-glycine running buffer, and Laemmli sample buffer with or without 50 mM dithiothreitol (DTT).

Human Fc receptors (FcγRI, FcγRIIIa, FcRn) were expressed with a C-terminal hexahistidine tag for affinity purification. Proteins were expressed as secreted components in Expi293 cells and purified by Ni-NTA affinity chromatography followed by preparative SEC.

2.2 | Electron microscopy

A 3.0-μL aliquot of 2Fc mAb at a concentration of 20 μg/mL was applied to glow discharged, 300 mesh Cu grids (Electron Microscopy Sciences) and stained with Nano-W (Nanoprobes). Data were collected using a Tecnai T12 transmission electron microscope operating at 120 keV. Images were taken using a Gatan 4 × 4 k CCD camera at a magnification of ×52 000 corresponding to a pixel size of 2.07 Å/pix. Particles were selected using interactive particle picking from ~100 micrographs in EMAN2 image processing suite.[22] A particle stack of ~10 000 particles was created and subjected to reference-free 2D classification to generate 50 classes. Representative classes are shown for clarity.

2.3 | Binding via the Fab domains

A 150 RU of each antibody (1Fc, 2Fc) in 10 mM citrate, pH 5.5, was covalently immobilized onto different flow cells of a CM5 chip (GE Life Sciences, 29104988) using

Biacore T200. At a flow rate of 50 μL/min, association with 10, 30, 90, 270, 810, or 2430 nM of CNTO7797 (mouse IgG1 anti-B21M idiotype) occurred for 90 seconds, followed by a 180-second dissociation step. Each concentration of CNTO7797 was performed in triplicate with double-reference subtraction. Running buffer was ×1 PBS, 0.05% (vol/vol) Tween 20, pH 7.2. Regeneration was performed using a 25-second pulse of 10 mM glycine, pH 2.0, at 20 μL/min, followed by a 30-second buffer wash and a 180-second stabilization period. Data were globally fit using the bivalent analyte model, with reported K_D values resulting from the first set of kinetic parameters, k_{a1} and k_{d1}.

2.4 | Effect of FcR density on mAb dissociation rate

Anti-6x-His Fab was generated from the full-length mAb using a Pierce Fab Micro Preparation Kit (Thermo Fisher, 44685) according to the manufacturer's instructions. A 3000 RU of anti-6x-His Fab in 10 mM citrate, pH 4.0, was covalently immobilized onto each of two flow cells of a CM5 sensor chip (GE Life Sciences, 29104988) using Biacore T200. At a flow rate of 50 μL/min, 1, 3, 10, 30, or 100 nM of His-tagged Fc receptor (FcγRI or FcRn) was captured to the surface for 60 seconds, followed by a 60-second association step with 10 nM anti-RSV 1Fc or 2Fc and a 300-second dissociation step. Each capture level (concentration of receptor) was performed in duplicate with double-reference subtraction. Running buffer was ×1 PBS, 0.05% (vol/vol) Tween 20 (pH 7.2 for FcγRI and pH adjusted to 6.0 using HCl for FcRn). Regeneration was performed using a 10-second pulse of 10 mM glycine, pH 1.5, at 20 μL/min, followed by a 180-second stabilization period. As some of the dissociation data did not fit well to a single exponential, two-point dissociation rates were calculated using the response at the beginning of the disassociation phase and after 300 (FcγRI) or 60 seconds (FcRn).

2.5 | FcR binding kinetics

A Biacore T200 instrument and CM5 chip containing anti-6x-His Fab (as above) were used for binding analysis. In separate experiments, 3 nM FcγRI, 10 nM FcγRIIIa, or 200 nM FcRn was captured onto the chip surface for 60 seconds, resulting in a capture level of 40, 50, and 100 RU, respectively. For FcγRI, association was performed using 1:3 serial dilutions of anti-RSV 1Fc or 2Fc (2–162 nM) for 90 seconds, followed by a 300-second dissociation. For FcγRIIIa, association was performed using 1:3 serial dilutions of anti-RSV 1Fc or 2Fc (12–3000 nM) for 60 seconds, followed by a 300-second dissociation. For FcRn, association was performed using 1:3 serial dilutions of anti-RSV 1Fc or 2Fc (1.2–300 nM) for 60 seconds, followed by a 180-second dissociation. Flow rate was 50 μL/min and running buffer was ×1 PBS, 0.05% (vol/vol) Tween 20 (pH 7.2 for FcγRI and FcγRIIIa and pH adjusted to 6.0 using HCl for FcRn). Regeneration was achieved with a 10-second pulse of 10 mM glycine, pH 1.5, at 20 μL/min, followed by a 180-second stabilization period. For consistency, each double-referenced dataset containing duplicates of each concentration was globally fit using the bivalent analyte model, with reported rates as the first set of kinetic parameters, k_{a1} and k_{d1}.

2.6 | FcR stoichiometry

CNTO6559 (anti-B21M idiotype) Fab was generated from the full-length mAb using a Pierce Fab Micro Preparation Kit (Thermo Fisher, 44685) according to the manufacturer's

instructions. 1500 RU of CNTO 6559 Fab in 10 mM citrate, pH 4.0, was covalently immobilized onto each of the two flow cells of a CM5 sensor chip (GE Life Sciences, 29104988) using Biacore T200. For FcγRI, 5 nM of anti-RSV 1Fc or 2Fc was captured via the Fab for 40 seconds in ×1 PBS, 0.05% (vol/vol) Tween 20, pH 7.2, followed by a 180-second association to 1:3 serial dilutions of FcγRI (0.12–30 nM) and a 300-second dissociation. For FcRn, 5 nM of anti-RSV 1Fc or 2Fc was captured via the Fab for 30 seconds in ×1 PBS, 0.05% (vol/vol) Tween 20 (pH adjusted to 6.0 using HCl), followed by a 180-second association to 1:3 serial dilutions of FcRn (4.1–1000 nM) and a 300-second dissociation. Each concentration of receptor was examined in duplicate at 50 μL/min with double-reference subtraction. Regeneration was performed using a 10-second pulse of 10 mM glycine, pH 1.5, at 20 μL/min, followed by a 180-second stabilization period. The response values were used to calculate the ratio of bound receptor to mAb at each concentration using the following equation:

$$\frac{\text{FcR}}{\text{mAb}} = \frac{\text{Response}}{\text{Capture level}} \div \frac{\text{MW}_{\text{FCR}}}{\text{MW}_{\text{mAb}}}$$

where Response is the binding response in RU achieved during the 180-second association, Capture level is the amount of mAb captured in RU, and MW is the molecular weight of the appropriate protein. Molecular weights were 150 027 Da for 1Fc, 204 335 Da for 2Fc, 40 096 Da for FcγRI, and 43 282 Da for FcRn. Note that the protein-only MW of FcγRI (30 843 Da) was multiplied by 1.3 to account for its high level of glycosylation.[23] The FcR:mAb ratio was then plotted as a function of [FcR] and fit to the hyperbolic binding equation,

$$\frac{\text{FcR}}{\text{mAb}} = \frac{B_{\max} \cdot [\text{FcR}]}{K_D + [\text{FcR}]}$$

where $B_{\max}$ is the maximal FcR:mAb stoichiometry and K_D is the equilibrium dissociation constant.

3 | RESULTS

3.1 | Design of 2Fc protein

In order to test whether a novel mAb scaffold containing two Fab and two Fc regions would have functional advantages compared to a wild-type mAb containing two Fabs and a single Fc region, we designed the 1Fc (wild-type) and 2Fc mAbs depicted in Figure 1 using the human IgG1 framework. Whereas 1Fc mAbs are composed of HCs and LCs, 2Fc mAbs can be generated by co-expression of a normal HC and a LC-Fc fusion. The DNA sequence of this fusion was designed by appending the hinge and Fc sequence from a normal HC to the C-terminus of the LC. Thus, rather than terminating at the end of the Fab sequence, the LC sequence continues for the formation of a second Fc region. These constructs were expressed using the variable sequences of an RSV mAb to create anti-RSV 1Fc and 2Fc mAbs.

3.2 | Purification and biochemical characterization

As expected, multiple protein products were obtained resulting from self-assembly of different combinations of the 2Fc mAb gene products in human embryonic kidney cells. After the initial protein A affinity chromatography step to purify Fc-containing proteins, it was evident that the desired 2Fc mAb had been formed along with additional products. SEC revealed the 200-kDa 2Fc mAb, as well as a 100-kDa protein (likely the monomeric version of 2Fc mAb containing one Fc and one Fab region) and some larger species representative of higher oligomers (Figure 2A). Nevertheless, separation via SEC could isolate the pure 200-kDa 2Fc product for further characterization.

In addition to analytical SEC, SDS-PAGE was used to verify the composition of the 2Fc mAb (Figure 2B). This species produced bands at 200 kDa under nonreducing conditions (assembled complex) and at 50 kDa under reducing conditions (HC and LC-Fc). The lack of intense bands below 200 kDa under nonreducing conditions indicates that disulfide bonds were primarily in the native, oxidized state. As a control, the 1Fc mAb showed bands at 150 kDa for the nonreduced complex and at 25 and 50 kDa for the reduced LC and HC.

3.3 | Structural and functional characterization

As a further probe of structural integrity, negative stain electron microscopy was performed on the 2Fc mAb (Figure 2C). 2D classification of particles selected from raw micrographs revealed four lobes of density equally dispersed from a central focus, resembling a tetrahedral architecture. This geometry is consistent with a protein that contains two each of Fc and Fab domains. Because this structure is distinct from that of standard IgGs or other published constructs, it was necessary to determine whether the function of the Fab region was altered. Therefore, we used an anti-idiotype mAb that targets the variable region of the anti-RSV mAbs to demonstrate that the 1Fc and 2Fc mAbs have similar binding via their Fab regions (Figure 2D,E). After fitting with the bivalent analyte model, the first set of kinetic parameters yielded K_D values of 639 ± 8 nM for the 1Fc mAb and 691 ± 3 nM for the 2Fc mAb. These data, combined with subsequent Fc binding experiments, support the predicted composition of the designed 2Fc mAb.

3.4 | Effect of FcR density on dissociation rate

mAbs achieve their high avidity for antigen, in part, due to bivalent binding of the two Fab regions to immobilized antigens, which allows for slow dissociation when both Fab arms are bound. Similarly, the 2Fc mAb was expected to dissociate from Fc receptors at a rate that is dependent upon receptor density; high levels of immobilized receptor allow for enhanced avidity due to bivalent binding and slower off rates. Thus, varying levels of FcR were captured onto a Biacore sensor chip surface, and binding parameters for their interaction with 1Fc and 2Fc mAbs were measured. The high-affinity Fcγ receptor I (FcγRI) was chosen to represent Fcγ receptors that bind IgG mAbs at the upper Fc region, and the FcRn was used to examine binding at its distal binding site at the C_H2-C_H3 interface of the Fc sequence.

For the 1Fc mAb, which was expected to bind FcγRs with the 1:1 stoichiometry typical of IgG mAbs,[24,25] there was no dependence of dissociation rate (k_d) on FcγRI capture density

(Figure 3A, Figure S1). In contrast, the k_d value for FcγRI-2Fc binding was strongly dependent on receptor capture level, with higher receptor density causing slower dissociation. For FcRn, both 1Fc and 2Fc mAbs showed kd values that were dependent on receptor density; however, the 2Fc mAb demonstrated consistently slower off rates (Figure 3B, Figure S1). Because each IgG HC contains an independent FcRn binding site,[26,27] multivalent binding and varying k_d values were expected for both 1Fc and 2Fc mAbs. The stronger dependence on receptor density for 2Fc indicates a higher avidity interaction.

3.5 | FcR binding kinetics

To determine equilibrium KD values of 1Fc and 2Fc mAbs for Fc receptors, an intermediate amount of receptor was captured and a full titration of varying mAb concentrations was performed. In addition to FcγRI and FcRn, FcγRIIIa V158 (high affinity variant) was analyzed due to its importance for ADCC. As some of these interactions contained multivalent molecules in solution, each dataset was fit with the bivalent analyte model for ease of comparison. Although both 1Fc and 2Fc mAbs bound with high affinity to FcγRI, the dissociation rate was significantly slower with 2Fc (Figure 4A,B). For FcγRIIIa, the 2Fc mAb displayed a significant increase in binding affinity over the 1Fc mAb, which was mediated mainly by its slower off rate (Figure 4C,D). FcRn binding at pH 6.0 was characterized by the same decrease in dissociation rate for the 2Fc mAb (Figure 4E,F). These data are summarized in Table 1 and demonstrate that the 2Fc mAb has a higher affinity for each surface-bound receptor, driven primarily by slower dissociation kinetics.

3.6 | FcR stoichiometry

As a final verification that the tighter Fc receptor binding of 2Fc was driven by its additional Fc region, experiments were devised to calculate the binding stoichiometry of 1Fc and 2Fc mAbs for FcRs. The 2Fc mAb was expected to bind twice the number of FcRs as the 1Fc mAb. Each mAb was captured to the surface of a Biacore chip via its Fab arms, and then the ratio of bound receptor to mAb was calculated when varying concentrations of FcRs were analyzed. The resulting hyperbolic fits provide the K_D value for mAbs binding to soluble Fc receptor and the capacity of receptor binding to captured mAb. As expected based on previous studies of IgG1 mAbs, the stoichiometry of the 1Fc mAb for Fc receptors was approximately 1:1 mAb:FcγRI (Figure 5A, Figure S2) and 1:2 mAb:FcRn (Figure 5B, Figure S2).[24–27] The 2Fc mAb bounds with double the stoichiometry to both FcγRI and FcRn, indicating that each Fc domain within the molecule is competent for receptor binding (Table 2). In terms of affinity, the 1Fc and 2Fc mAbs had very similar K_D values for soluble FcγRI and FcRn. Thus, the enhancement in affinity of 2Fc for FcRs noted previously requires receptor immobilization for the avidity effect to occur.

4 | DISCUSSION

Here, we describe the design and characterization of a novel mAb framework using the human IgG1 scaffold, which contains two functional Fc regions in addition to its two Fabs. The 2Fc mAb was straightforward to produce, with just one SEC step required after protein A affinity chromatography. The 2Fc mAb had the expected structural properties, including a mass of ~200 kDa and the presence of four discrete domains. Functionally, the 2Fc mAb

retained binding activity via its Fab domains and had greatly enhanced avidity to surface-immobilized Fc receptors.

Several protein products may possibly form after cotransfection of plasmid DNA containing mAb HC and LC-Fc fusion genes; however, routine purification strategies were sufficient to obtain pure 2Fc mAb. The observed 100-kDa contaminant likely corresponds to HC-LC heterodimer but could feasibly be HC or LC-Fc homodimer. LC dimers have been observed in the context of Bence-Jones proteins, where the hydrophobic sequence of certain V_L regions drives their association.[28] LCs with different variable regions have a wide range of dimerization propensities, with K_D values ranging over 1000-fold depending on the identity of residues in the complementarity-determining regions.[29] The formation of LC dimer-related contaminants would also potentially increase in cases where the LC-Fc plasmid is more efficiently transfected or expressed than the HC plasmid.[30] Conversely, cell secretion of HC dimers has been observed for some engineered mAbs in the absence of paired LC and could also contribute to the 100-kDa fraction.[31] However, the strong affinity of the native HC-LC interaction would presumably favor the formation of heterodimers rather than homodimers. As for the purified 200-kDa species, the correct chain composition (H_2L_2) is supported by full retention of binding capacity via the Fab domains. If HC or LC-Fc homodimer contaminants were present (eg, H_4, H_3L, HL_3, L_4), binding to anti-idiotype mAb would have been disrupted. If required, purification steps based on affinity capture of both HC (eg, anti-C_H1 resin) and LC (eg, protein L resin) could be used to increase purity of the desired species, as can chromatographies based on ion exchange or hydrophobic interactions.

Other mAb frameworks utilizing Fc multimerization strategies have shown augmented effector functions including ADCP, ADCC, and opsonophagocytic killing.[19–21] These tandem Fc proteins are similar to the 2Fc mAb in terms of size, biochemical properties, and improvement of FcγR binding. The major difference is that previous work has used tandemly linked Fc domains, while the 2Fc framework described in this work creates a branched, tetrahedral-like structure, or other geometry. It is possible that this unique geometry would allow for distinct cross-linking properties. Specifically, the 2Fc arrangement of Fc domains may mimic the cross-linking ability of the two Fab domains, allowing for receptor clustering and improved effector functions. Stoichiometric studies demonstrating the capacity of 2Fc mAbs to interact simultaneously with multiple Fc receptors lend credence to this hypothesis. The previously unexplored geometry of 2Fc mAbs could differentially impact Fc receptor binding, providing a potential strategy to tune the recruitment of various immune cells and elicit distinct immune responses. Further studies are required to determine ADCC and ADCP functions of the 2Fc construct.

mAb constructs with multiple Fc stem regions have been considered previously. Roche's DuoMAbs, distinct 2Fc mAbs prepared using CrossMAb technology, are structurally similar to the 2Fc mAbs investigated here.[32] That framework had been briefly described in a review and described in a publicly available patent application.[32,33] While our work was under review for publication, a complete characterization of DuoMAbs was published.[34] Structurally, the DuoMAbs may be more planar than tetrahedral, which may also be the case for our dual Fc. It appears that DuoMAbs share many functional features of the 2Fc mAbs

presented here and also have enhanced ADCC activity, thus providing proof-of-principle that molecules with two Fc regions could more effectively interact with FcγRIII receptors in vivo. Despite the similarities, DuoMAbs are distinct from our dual Fc in primary sequence since they have the C_H1-C_L domain swap typical of the CrossMAb framework. This change makes the sequence slightly less native and necessitates additional cloning efforts.

In the future, the in vitro and in vivo activity of this 2Fc mAb could be assessed to determine whether the observed increase in binding avidity has functional consequences at physiological densities of FcR. This would likely necessitate the use of 2Fc proteins that target antigens expressed on tumor cells, such as CD20 or epidermal growth factor receptor. Because the 2Fc mAb has enhanced FcR binding only at sufficient receptor density, it is important to consider the type of effector cells used in these experiments. Larger differences in mAb activity may be observed using polymorphonuclear neutrophils, which express high levels of FcγRIII arranged in topographical ridges and folds.[35] Although NK cells are more frequently employed to assess ADCC, use of neutrophils is also therapeutically relevant given their high abundance in blood. Ultimately, experiments in animal models would demonstrate whether the enhancement of FcγR and FcRn binding observed here in vitro affects in vivo properties like control of tumor growth and mAb pharmacokinetics.

Previously, mAbs containing an IgG1 and IgA2 Fc linked in tandem were shown to have enhanced neutrophil-mediated ADCC compared to mAbs containing IgG or IgA Fc alone, which resulted from binding of FcαRI in addition to FcγRs.[36] This combination of distinct functions based on incorporation of multiple Fc types could be similarly achieved using the 2Fc format. Because 2Fc mAbs use the normal IgG HC, the only required cloning is fusion of the new Fc region onto the C-terminus of the normal LC. Another derivation would be to create bispecific 2Fc molecules using established HC-HC and HC-LC pairing strategies.[37] These same protein engineering methods may also help to improve the yield of the 2Fc protein relative to the 100-kDa side product. Thus, while the 2Fc framework on its own increases receptor-binding avidity, it could also be combined with other protein engineering strategies to create molecules with novel or improved therapeutic functions. The work described here provides a strategy to produce new IgG-based constructs with multiple Fc regions that could be further engineered for desired functionality.

Supplementary Material

Refer to Web version on PubMed Central for supplementary material.

ACKNOWLEDGMENTS

This work was supported by the University of Washington, Department of Medicinal Chemistry, and National Institutes of Health T32GM007750.

Funding information

National Institutes of Health, Grant/Award Number: T32GM007750; University of Washington

REFERENCES

1. Ecker DM, Jones SD, Levine HL. The therapeutic monoclonal antibody market. MAbs. 2015;7(1):9–14. https://doi.org/104161/19420862.2015.989042. [PubMed: 25529996]
2. Kaplon H, Reichert JM. Antibodies to watch in 2019. MAbs. 2019;11 (2):219–238. 10.1080/19420862.2018.1556465. [PubMed: 30516432]
3. Weiner GJ. Building better monoclonal antibody-based therapeutics. Nat Rev Cancer. 2015;15(6):361–370. https://doiorg/10.1038/nrc3930. [PubMed: 25998715]
4. Redman JM, Hill EM, AlDeghaither D, Weiner LM. Mechanisms of action of therapeutic antibodies for cancer. Mol Immunol. 2015;67 (2A):28–45. 10.1016/j.molimm.2015.04.002. [PubMed: 25911943]
5. Vidarsson G, Dekkers G, Rispens T. IgG subclasses and allotypes: from structure to effector functions. Front Immunol. 2014;5:520 10.3389/fimmu.2014.00520. [PubMed: 25368619]
6. Roopenian DC, Akilesh S. FcRn: the neonatal fc receptor comes of age.Nat Rev Immunol. 2007;7(9):715–725. 10.1038/nri2155. [PubMed: 17703228]
7. Kellner C, Otte A, Cappuzzello E, Klausz K, Peipp M. Modulating cytotoxic effector functions by fc engineering to improve cancer therapy. Transfus Med Hemotherapy. 2017;44(5):327–336. 10.1159/000479980.
8. Wang X, Mathieu M, Brezski RJ. IgG fc engineering to modulate antibody effector functions. Protein Cell. 2018;9(1):63–73. 10.1007/s13238-017-0473-8. [PubMed: 28986820]
9. Alegre M-L, Collins AM, Pulito VL, et al. Effect of a single amino acid mutation on the activating and immunosuppressive properties of a “humanized” OKT3 monoclonal antibody. J Immunol. 1992;148(11): 3461–3468. http://www.ncbi.nlm.nih.gov/pubmed/1534096. [PubMed: 1534096]
10. Vafa O, Gilliland GL, Brezski RJ, et al. An engineered fc variant of an IgG eliminates all immune effector functions via structural perturbations. Methods. 2014;65(1):114–126. 10.1016/j.ymeth.2013.06.035. [PubMed: 23872058]
11. Richards JO, Karki S, Lazar GA, Chen H, Dang W, Desjarlais JR. Optimization of antibody binding to FcγRIIa enhances macrophage phagocytosis of tumor cells. Mol Cancer Ther. 2008;7(8):2517–2527. 10.1158/1535-7163.MCT-08-0201. [PubMed: 18723496]
12. Shields RL, Namenuk AK, Hong K, et al. High resolution mapping of the binding site on human IgG1 for FcγRI, FcγRII, FcγRIII, and FcRn and design of IgG1 variants with improved binding to the FcγR. J Biol Chem. 2001;276(9):6591–6604. 10.1074/jbc.M009483200. [PubMed: 11096108]
13. Lazar GA, Dang W, Karki S, et al. Engineered antibody fc variants with enhanced effector function. Proc Natl Acad Sci. 2006;103(11):4005–4010. 10.1073/pnas.0508123103. [PubMed: 16537476]
14. Liu Z, Gunasekaran K, Wang W, et al. Asymmetrical fc engineering greatly enhances antibody-dependent cellular cytotoxicity (ADCC) effector function and stability of the modified antibodies. J Biol Chem. 2014;289(6):3571–3590. 10.1074/jbc.M113.513366. [PubMed: 24311787]
15. Tam SH, McCarthy SG, Armstrong AA, et al. Functional, biophysical, and structural characterization of human IgG1 and IgG4 fc variants with ablated immune functionality. Antibodies. 2017;6(3):12 10.3390/antib6030012.
16. Shields RL, Lai J, Keck R, et al. Lack of fucose on human IgG1 N-linked oligosaccharide improves binding to human FcγRIII and antibody-dependent cellular toxicity. J Biol Chem. 2002;277(30):26733–26740. 10.1074/jbc.M202069200. [PubMed: 11986321]
17. Diebolder CA, Beurskens FJ, de Jong RN, et al. Complement is activated by IgG hexamers assembled at the cell surface. Science. 2014; 343(6176):1260–1263. 10.1126/science.1248943. [PubMed: 24626930]
18. Cook EM, Lindorfer MA, van der Horst H, et al. Antibodies that efficiently form hexamers upon antigen binding can induce complement-dependent cytotoxicity under complement-limiting conditions. J Immunol. 2016;197(5):1762–1775. 10.4049/jimmunol.1600648. [PubMed: 27474078]
19. Nagashima H, Tezuka T, Tsuchida W, Maeda H, Kohroki J, Masuho Y. Tandemly repeated fc domain augments binding avidities of antibodies for Fcγ receptors, resulting in enhanced

antibody-dependent cellular cytotoxicity. Mol Immunol. 2008;45(10):2752–2763. 10.1016/j.molimm.2008.02.003. [PubMed: 18353438]

20. Nagashima H, Ootsubo M, Fukazawa M, Motoi S, Konakahara S, Masuho Y. Enhanced antibody-dependent cellular phagocytosis by chimeric monoclonal antibodies with tandemly repeated fc domains. J Biosci Bioeng. 2011;111(4):391–396. 10.1016/j.jbiosc.2010.12.007. [PubMed: 21215693]
21. Wang Q, Chen Y, Pelletier M, et al. Enhancement of antibody functions through fc multiplications. MAbs. 2017;9(3):393–403. 10.1080/19420862.2017.1281505. [PubMed: 28102754]
22. Tang G, Peng L, Baldwin PR, et al. EMAN2: an extensible image processing suite for electron microscopy. J Struct Biol. 2007;157(1): 38–46. 10.1016/j.jsb.2006.05.009. [PubMed: 16859925]
23. Hayes JM, Cosgrave EFJ, Struwe WB, et al. Glycosylation and fc receptors. Curr Top Microbiol Immunol. 2014;382:165–199. 10.1007/978-3-319-07911-0_8. [PubMed: 25116100]
24. Kiyoshi M, Caaveiro JMM, Kawai T, et al. Structural basis for binding of human IgG1 to its high-affinity human receptor FcγRI. Nat Commun. 2015;6:6866 10.1038/ncomms7866. [PubMed: 25925696]
25. Radaev S, Sun P. Recognition of immunoglobulins by Fcγ receptors.Mol Immunol. 2002;38(14):1073–1083. 10.1016/S0161-5890(02)00036-6. [PubMed: 11955599]
26. Sánchez LM, Penny DM, Bjorkman PJ. Stoichiometry of the interaction between the major histocompatibility complex-related fc receptor and its fc ligand. Biochemistry. 1999;38(29):9471–9476. 10.1021/bi9907330. [PubMed: 10413524]
27. Abdiche YN, Yeung YA, Chaparro-Riggers J, et al. The neonatal fc receptor (FcRn) binds independently to both sites of the IgG homodimer with identical affinity. MAbs. 2015;7(2):331–343. 10.1080/19420862.2015.1008353. [PubMed: 25658443]
28. Kaplan B, Livneh A, Sela B-A. Immunoglobulin free light chain dimers in human diseases. Sci World J. 2011;11:726–735. 10.1100/tsw.2011.65.
29. Stevens FJ, Westholm FA, Solomon A, Schiffer M. Self-association of human immunoglobulin κI light chains: role of the third hypervariable region. Proc Natl Acad Sci U S A. 1980;77(2):1144–1148. 10.1073/pnas.77.2.1144. [PubMed: 6767243]
30. Spooner J, Keen J, Nayyar K, et al. Evaluation of strategies to control fab light chain dimer during mammalian expression and purification: a universal one-step process for purification of correctly assembled fab. Biotechnol Bioeng. 2015;112(7):1472–1477. 10.1002/bit.25550. [PubMed: 25619171]
31. Stoyle CL, Stephens PE, Humphreys DP, Heywood S, Cain K, Bulleid NJ. IgG light chain-independent secretion of heavy chain dimers: consequence for therapeutic antibody production and design. Biochem J. 2017;474(18):3179–3188. https://doiorg/10.1042/BCJ20170342. [PubMed: 28784690]
32. Klein C, Schaefer W, Regula JT. The use of CrossMAb technology for the generation of bi- and multispecific antibodies. MAbs. 2016;8(6): 1010–1020. 10.1080/19420862.2016.1197457. [PubMed: 27285945]
33. Bossenmaier B, Kettenberger H, Klein C, et al. Wo2012116926a1: Antigen Binding Proteins. 2012.
34. Sustmann C, Dickopf S, Regula JT, et al. DuoMab: a novel CrossMab-based IgG-derived antibody format for enhanced antibody-dependent cell-mediated cytotoxicity. MAbs. 2019;11(8):1–13. 10.1080/19420862.2019.1661736.
35. Fernández-Segura E, García JM, López-Escámez JA, Campos A. Surface expression and distribution of fc receptor III (CD16 molecule) on human natural killer cells and polymorphonuclear neutrophils. Microsc Res Tech. 1994;28(4):277–285. 10.1002/jemt.1070280404. [PubMed: 7919518]
36. Borrok MJ, Luheshi NM, Beyaz N, et al. Enhancement of antibody-dependent cell-mediated cytotoxicity by endowing IgG with FcαRI (CD89) binding. MAbs. 2015;7(4):743–751. 10.1080/19420862.2015.1047570. [PubMed: 25970007]
37. Brinkmann U, Kontermann RE. The making of bispecific antibodies. MAbs. 2017;9(2):182–212. 10.1080/19420862.2016.1268307 [PubMed: 28071970]

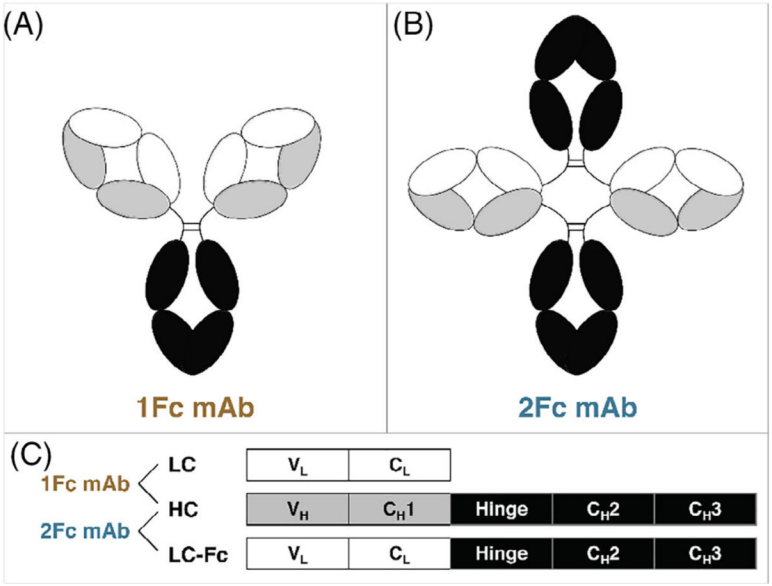

FIGURE 1.

Design of 1Fc and 2Fc mAbs. Whereas 1Fc mAb (A) contains the native configuration of two Fabs and one Fc region, 2Fc mAb (B) contains two each of Fab and Fc regions. C, Proteins were produced in HEK293 cells using expression plasmids containing the sequences for the mAb heavy and light chains (1Fc) or heavy chain and light chain-Fc fusion (2Fc). Fab, antigen-binding fragment; Fc, crystallizable fragment; HEK, human embryonic kidney; mAb, monoclonal antibody

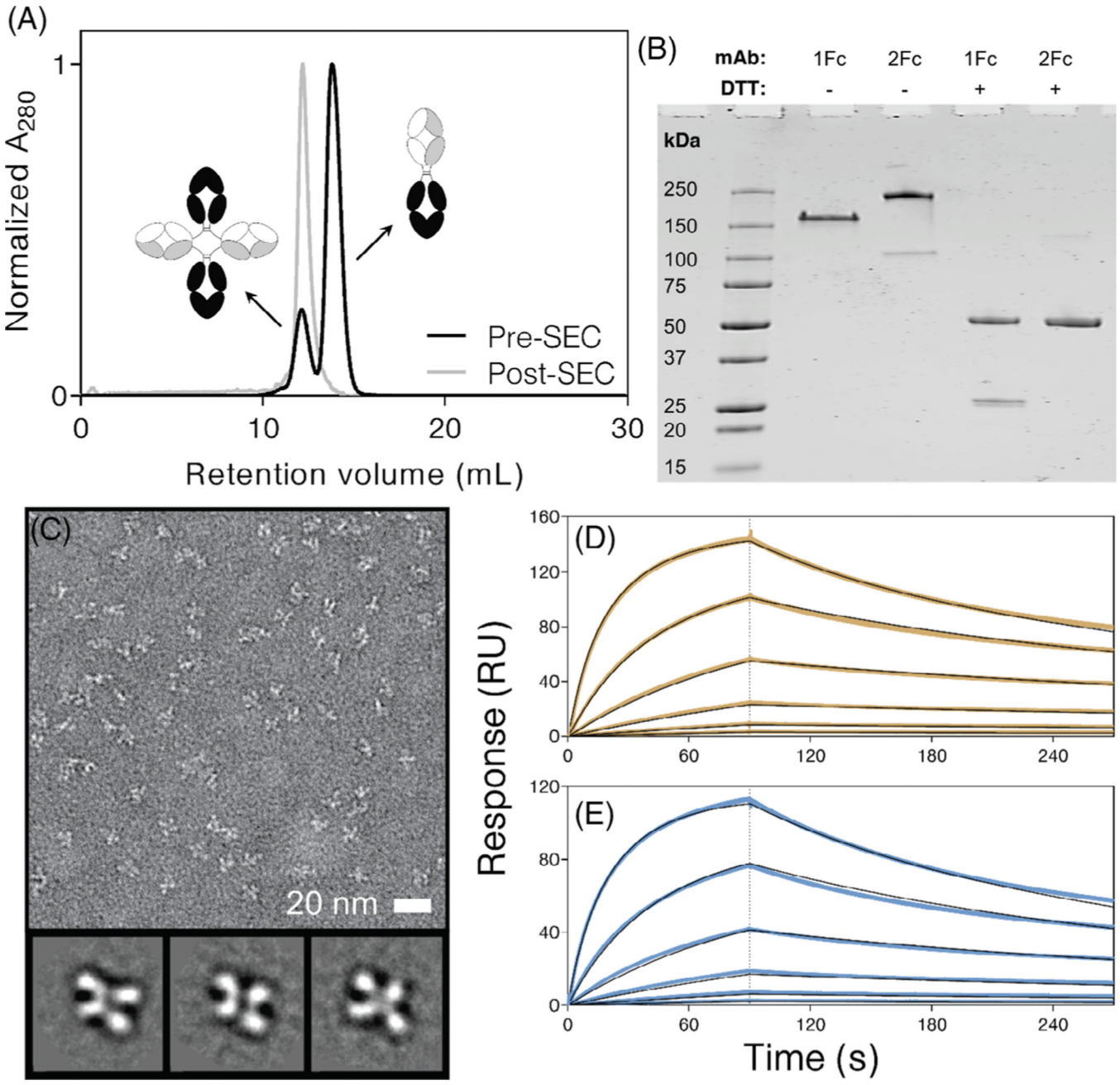

FIGURE 2.

Biochemical characterization of 1Fc and 2Fc proteins. After protein A purification, 2Fc mAb was purified by SEC (A), where the desired 2Fc species was separated from an excess of smaller contaminants of half the molecular weight. Preparative SEC data of the initial sample (black) are shown along with analytical SEC data of the purified 2Fc protein (gray). After purification, 1Fc and 2Fc proteins were analyzed by nonreducing (−DTT) and reducing (+DTT) SDS-PAGE (B). Under nonreducing conditions, full-length proteins were observed as primary bands at 150 kDa for 1Fc and 200 kDa for 2Fc. Under reducing conditions, bands for free heavy chain (50 kDa) and light chain (25 kDa) were observed for

1Fc while overlapping bands at 50 kDa represent the heavy chain and light chain-Fc components of the 2Fc mAb. The 2Fc protein was visualized using electron microscopy (C) where selected classifications show the predicted 3D structure containing four lobes of density. Intact function of the variable regions was demonstrated based on SPR of 1Fc (D) and 2Fc (E) mAbs binding to anti-idiotype antibody. Triplicate data (1Fc, brown; 2Fc, blue) were globally fit to the bivalent analyte model (fits shown as black lines). DTT, dithiothreitol; Fab, antigen-binding fragment; Fc, crystallizable fragment; mAb, monoclonal antibody; SEC, size-exclusion chromatography

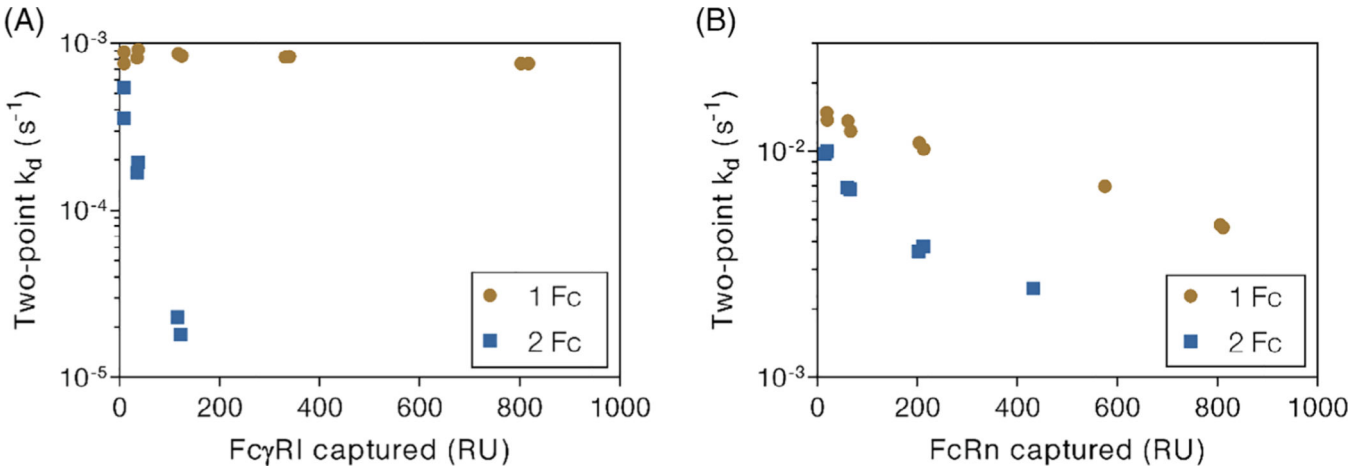

FIGURE 3.

Effect of FcR density on mAb dissociation rate. Varying levels of His-tagged FcγRI (A) or FcRn (B) were captured to a CM5 sensor chip which contained immobilized anti-His Fab. Following FcR capture, association with 10 nM 1Fc or 2Fc mAb was performed, followed by a 300-second dissociation phase. The running buffer was ×1 PBS, pH 7.2, for FcγRI and ×1 PBS, pH 6.0, for FcRn. Two-point FcR-mAb dissociation rates (k_d values) were calculated based on the binding response at the beginning of the dissociation phase and the response after 60 (FcRn) or 300 (FcγRI) seconds of dissociation. Each point shows an individual replicate for 1Fc (brown circles) or 2Fc (blue squares). Surface plasmon resonance (SPR) sensorgrams are shown in Figure S1. Fab, antigen-binding fragment; Fc, crystallizable fragment; FcRn, neonatal Fc receptor; mAb, monoclonal antibody; PBS, phosphate-buffered saline

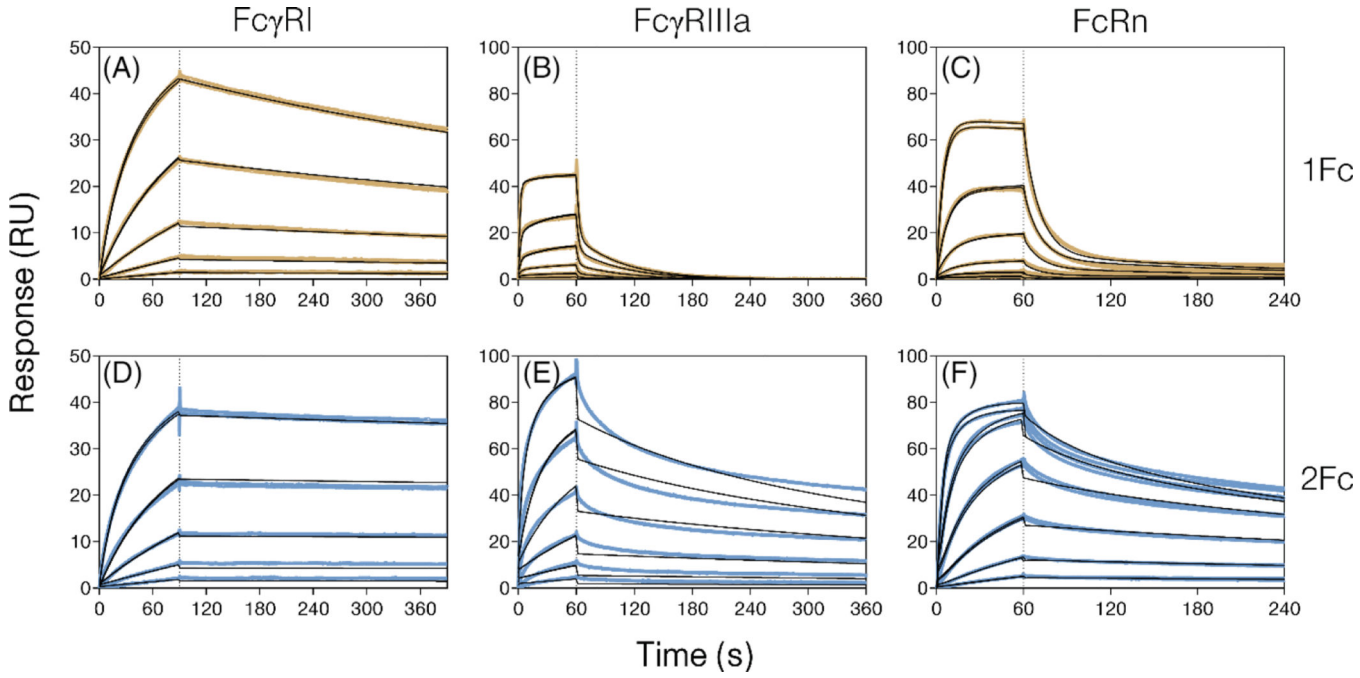

FIGURE 4.

Kinetics of 1Fc and 2Fc mAbs binding to captured FcRs. A low level of FcγRI (A, B), FcγRIIIa (C, D), or FcRn (E, F) was captured to the surface of a CM5 sensor chip using immobilized anti-His Fab. The FcRs were then associated with 3-fold serial dilutions of 1Fc (A, C, E) or 2Fc (B, D, F) mAb followed by a dissociation phase. Final mAb concentrations were 2–162 nM (FcγRI), 12–3000 nM (FcγRIIIa), or 1.2–300 nM (FcRn), and the running buffer was ×1 PBS, pH 7.2 (FcγRI, FcγRIIIa) or ×1 PBS, pH 6.0 (FcRn). Data were globally fit to the bivalent analyte model in Biacore T200 Evaluation Software, with the k_{a1} and k_{d1} values reported in Table 1. Each duplicate measurement is shown in brown (1Fc) or blue (2Fc) with fitted lines in black. Fab, antigen-binding fragment; Fc, crystallizable fragment; FcRn, neonatal Fc receptor; mAb, monoclonal antibody; PBS, phosphate-buffered saline

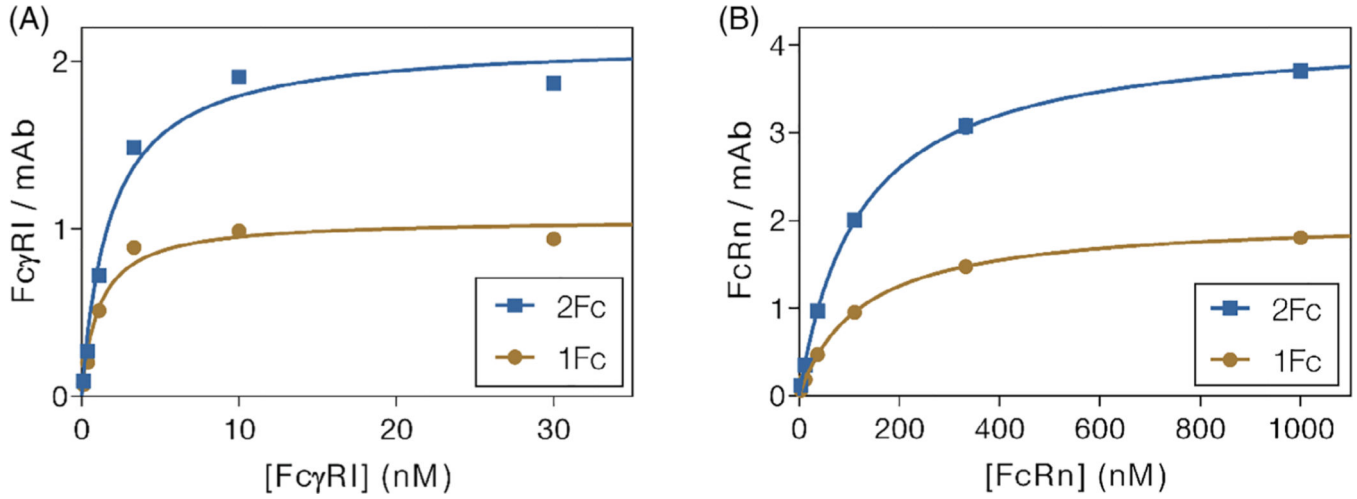

FIGURE 5.

Stoichiometry of mAb-FcR binding. 1Fc or 2Fc mAb was captured to the surface of a CM5 sensor chip via the Fab arms using an immobilized anti-idiotype Fab, leaving the Fc region exposed for FcR binding. The captured mAb was then associated with FcγRI (A) or FcRn (B), followed by a dissociation phase. The binding response 4 seconds before the end of the association phase, along with the mAb capture level and protein molecular weights, was used to plot the number of FcR molecules bound to each mAb molecule at each FcR concentration based on the equation described in the methods. Each duplicate measurement is shown in brown circles (1Fc) or blue squares (2Fc), and fits to the hyperbolic binding equation are plotted in a line of matching color. Fit parameters N and K_D are listed in Table 2, and SPR sensorgrams are shown in Figure S2. Fab, antigen-binding fragment; Fc, crystallizable fragment; FcRn, neonatal Fc receptor; mAb, monoclonal antibody

TABLE 1

Kinetic parameters for 1Fc and 2Fc mAbs binding to captured Fc receptors

Receptor	Antibody	[a] k_a (M^{-1} s^{-1})	1Fc/2Fc k_a	[a] k_d (s^{-1})	1Fc/2Fc k_d	K_D (nM)	1Fc/2Fc K_D
FcγRI	1Fc	76 600 ± 200	0.87	0.00128 ± 0.00001	6.2	16.7 ± 0.1	7.1
	2Fc	87 800 ± 300		0.000207 ± 0.000002		2.36 ± 0.02	
FcγRIIIa	1Fc	51 300 ± 200	3.2	0.4682 ± 0.002	130	9130 ± 50	42
	2Fc	15 900 ± 100		0.00349 ± 0.00002		219 ± 2	
FcRn	1Fc	218 000 ± 1000	0.25	0.0872 ± 0.0003	8.9	400 ± 2	35
	2Fc	860 000 ± 1000		0.00980 ± 0.00008		11.4 ± 0.1	

Abbreviations: Fc, crystallizable fragment; FcRn, neonatal Fc receptor; mAb, monoclonal antibody.

[a] k_a and k_d values shown are the first set of kinetic parameters from bivalent analyte fits.

TABLE 2

Stoichiometry and affinity of 1Fc and 2Fc mAbs binding to soluble Fc receptors

Receptor	Antibody	*N*	2Fc/1Fc *N*	K_D (nM)	1Fc/2Fc K_D
FcγRI	1Fc	1.06 ± 0.04	2.0	1.11 ± 0.18	1.6
	2Fc	2.12 ± 0.08		1.82 ± 0.25	
FcRn	1Fc	2.03 ± 0.02	2.1	124 ±4	1.0
	2Fc	4.17 ± 0.05		121 ±4	

Abbreviations: Fc, crystallizable fragment; FcRn, neonatal Fc receptor; mAb, monoclonal antibody.